Formation of heavy neutron-rich nuclei by ^{48}Ca-induced multinucleon transfer reactions

Zhi Cheng (成智) and Xiao Jun Bao (包小军)*

Department of Physics, Collaborative Innovation Center for Quantum Effects, and Key Laboratory of Low Dimensional Quantum Structures and Quantum Control of Ministry of Education, Hunan Normal University, Changsha 410081, People's Republic of China

(Received 20 October 2020; accepted 8 February 2021; published 25 February 2021)

The reaction systems ^{48}Ca + ^{238}U and ^{48}Ca + ^{248}Cm are investigated within the improved dinuclear system model+GEMINI++. The theoretical results show that the distributions of isotopes in the ^{48}Ca + ^{238}U reaction are well described with the model. For the ^{48}Ca + ^{248}Cm reaction, the model partly describes well the experimental production cross sections. Experimental and theoretical data from multinucleon transfer reactions indicate that the isotopic distributions of the ^{48}Ca + ^{238}U reaction system above Pb are shifted toward the neutron-rich side as compared to the ^{136}Xe + ^{208}Pb reaction except the isotopic distribution of Bi.

DOI: 10.1103/PhysRevC.103.024613

I. INTRODUCTION

Multinucleon transfer (MNT) reactions of actinide targets ranging from U to Cf with various projectiles ranging from ^{18}O to ^{238}U have been extensively studied [1–4]. The original motivation for studying MNT reactions with actinide targets is to establish a pathway to produce superheavy nuclei. From these studies it was found that transfer reactions could provide a means of synthesizing other actinide nuclides and unknown heavy neutron-rich isotopes [4–7]. Recently, the synthesis of heavy neutron-rich nuclei in the laboratory has been greatly inspired using MNT reactions [8–21].

A large number of theoretical approaches [22–53] have been developed to describe the MNT process, the model based on the concept of the dinuclear system (DNS) is one of them [26,27,31–34,42,44,45]. Recently, the evolution of DNS is regarded as a diffusion process by taking the deformation of the interaction nuclei as an independent variable and solving the master equation of four variables [54]. This improved DNS model [54–56] has been so far successfully applied in the description of fusion reactions as well as MNT reactions with Pb or Pt as the target material.

In this paper, we adopted the improved DNS model for the description of MNT reactions with ^{48}Ca bombarded actinide targets and for the prediction of the corresponding transfer cross sections. To test our calculated abilities on the transfer cross sections using the DNS model+GEMINI++, our studies for all investigations were performed with one set of parameters and with the same assumptions [55]. The main purpose of this work is to demonstrate the accuracy of the present method, the reaction systems ^{48}Ca + ^{238}U and ^{48}Ca + ^{248}Cm are investigated and compared with experimental data. The calculated cross sections for the production of heavy neutron-rich nuclei (Z = 83–91) in the ^{48}Ca + ^{238}U reaction have been compared with those predicted in the ^{136}Xe + ^{208}Pb reaction. The aim of this comparison is to get information if Pb or actinide targets are more profitable to reach heavy neutron-rich isotopes.

II. THEORETICAL FRAMEWORK

Multinucleon rearrangement process can be described as a diffusion process by numerically solving a set of four-variable master equations (MEs) in the corresponding potential energy surface (PES) [55]. The time evolution of the probability distribution function $P(Z_1, N_1, \beta_1, \beta_2, t)$ for fragment 1 with Z_1, N_1, β_1, and β_2 at time t is described by the following master equations [56]:

$$\begin{aligned}
&\frac{dP(Z_1, N_1, \beta_1, \beta_2, t)}{dt} \\
&= \sum_{Z_1'} W_{Z_1,N_1,\beta_1,\beta_2;Z_1',N_1,\beta_1,\beta_2}(t)\big[d_{Z_1,N_1,\beta_1,\beta_2}P(Z_1', N_1, \beta_1, \beta_2, t) \\
&\quad - d_{Z_1',N_1,\beta_1,\beta_2}P(Z_1, N_1, \beta_1, \beta_2, t)\big] \\
&\quad + \sum_{N_1'} W_{Z_1,N_1,\beta_1,\beta_2;Z_1,N_1',\beta_1,\beta_2}(t) \\
&\quad \times \big[d_{Z_1,N_1,\beta_1,\beta_2}P(Z_1, N_1', \beta_1, \beta_2, t) \\
&\quad - d_{Z_1,N_1',\beta_1,\beta_2}P(Z_1, N_1, \beta_1, \beta_2, t)\big] \\
&\quad + \sum_{\beta_1'} W_{N_1,Z_1,\beta_1,\beta_2;N_1,Z_1,\beta_1',\beta_2}(t) \\
&\quad \times \big[d_{Z_1,N_1,\beta_1,\beta_2}P(Z_1, N_1, \beta_1', \beta_2, t) \\
&\quad - d_{Z_1,N_1,\beta_1',\beta_2}P(Z_1, N_1, \beta_1, \beta_2, t)\big] \\
&\quad + \sum_{\beta_2'} W_{N_1,Z_1,\beta_1,\beta_2;N_1,Z_1,\beta_1,\beta_2'}(t) \\
&\quad \times \big[d_{Z_1,N_1,\beta_1,\beta_2}P(Z_1, N_1, \beta_1, \beta_2', t) \\
&\quad - d_{Z_1,N_1,\beta_1,\beta_2'}P(Z_1, N_1, \beta_1, \beta_2, t)\big],
\end{aligned} \tag{1}$$

*baoxiaojun@hunnu.edu.cn

where $W_{Z_1,N_1,\beta_1,\beta_2;Z_1',N_1,\beta_1,\beta_2}$ is the average transition probability from channels $(Z_1', N_1, \beta_1, \beta_2)$ to $(Z_1, N_1, \beta_1, \beta_2)$. d_{N_1,Z_1} represents the microscopic dimension of the macroscopic state $(N_1, Z_1, \beta_1, \beta_2)$ [57,58]. The β_1 and β_2 denote quadrupole deformations of fragments, they are considered as two discrete variables, corresponding to the projectile-like and target-like fragments (TLFs), respectively. Some details is addressed in Refs. [54–56].

The potential energy surface of DNS model is determined by [55]

$$\begin{aligned} U(N_1, Z_1, N_2, Z_2, R_{\rm cont}, \beta_1, \beta_2, J) &= B(N_1, Z_1, \beta_1) + B(N_2, Z_2, \beta_2) \\ &+ V_{\rm CN}(N_1, Z_1, N_2, Z_2, R_{\rm cont}, \beta_1, \beta_2) \\ &+ V_{\rm rot}(N_1, Z_1, N_2, Z_2, R_{\rm cont}, \beta_1, \beta_2, J), \end{aligned} \tag{2}$$

where $N = N_1 + N_2$ and $Z = Z_1 + Z_2$, the β_1 and β_2 represent quadrupole deformations of the two fragments, respectively. The nucleon transfer process takes places can be assumed by $R_{\rm cont} = R_1(1 + \beta_1 Y_{20}(\theta_1)) + R_2(1 + \beta_2 Y_{20}(\theta_2)) + 0.5$ fm, with $R_i = 1.16A_i^{1/3}$ [55]. The $B(N_1, Z_1, \beta_1)$ and $B(N_2, Z_2, \beta_2)$ are the binding energies of two deformed nuclei [59,60], respectively.

The cross section of the production of a primary fragment is written as a sum over all partial waves J:

$$\sigma^{\rm pri}_{Z_1,N_1}(E_{\rm c.m.}) = \frac{\pi\hbar^2}{2\mu E_{\rm c.m.}} \sum_J (2J+1) T(E_{\rm c.m.}, J) \times \sum_{\beta_1,\beta_2} P(Z_1, N_1, \beta_1, \beta_2, J, \tau_{\rm int}), \tag{3}$$

where the penetration coefficient $T(E_{\rm c.m.}, J)$ is assumed when the incident energy is higher than the interaction barrier, $T(E_{\rm c.m.}, J)$ is estimated to be 1, while to be 0 for other cases.

The production cross sections of the final fragments in transfer reactions can be written as

$$\sigma^{\rm fin}_{Z_1,N_1}(E_{\rm c.m.}) = \sum_{Z_1',N_1'J'} \sigma^{\rm pri}(Z_1', N_1', J') \times P(Z_1, N_1; Z_1', N_1', J'). \tag{4}$$

It is assumed that the sharing of the total excitation energy between the target-like and projectile-like fragments are proportional to their masses $E^*_{Z_1,N_1} = E_{\rm tot} \times A_1/(A_1 + A_2)$, where A_1, A_2 are the corresponding mass number. The code GEMINI++ is used to calculate the sequential statistical evaporation of excited fragments [61–63].

III. NUMERICAL RESULTS AND DISCUSSIONS

In order to test the model, the transfer cross sections by using the reaction ^{48}Ca + ^{238}U have been performed at incident energy $E_{\rm c.m.} = 195.00$ MeV. Transfer cross sections according to the change of the proton number of the target-like fragment (TLF) from ^{238}U as functions of the neutron number of the TLF are shown in Fig. 1. It can be seen that the agreement between the calculated and experimental data [64] is reasonably good taking into consideration the experimental uncertainties. This results indicates that the improved DNS model is applicable for the study of multinucleon transfer reactions near the barrier energies.

In Fig. 1, one can see that the calculated distributions of final fragments as compared to the distributions of primary fragments are shifted by 6–8 neutrons for more proton transfers ($-7p$ to $-11p$). That is because positive reaction Q value of projectile-like and target-like fragments acts to increase the excitation energy of the primary products. However, the Pb region nuclei compared to actinide nuclei which have lower fission barriers [65], this leads to the high survivability of these nuclei against fission. Therefore, the primary fragments

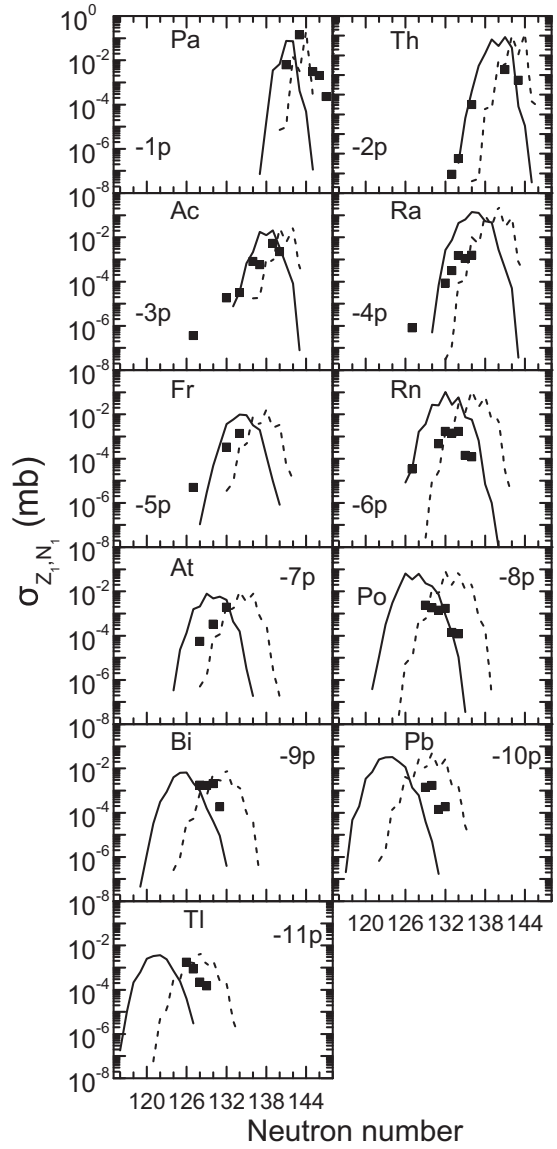

FIG. 1. Transfer cross sections for the ^{48}Ca + ^{238}U reaction at $E_{\rm c.m.} = 195.00$ MeV. The number of transferred protons from ^{238}U to ^{48}Ca is indicated. The measured cross sections are taken from Ref. [64]. The black dotted line represents the primary product distribution cross section and the black solid line represents the final product distribution cross section. Black solid points represent experimental data. Here, the negative number of transferred nucleons denotes the number of nucleons removed from the projectile.

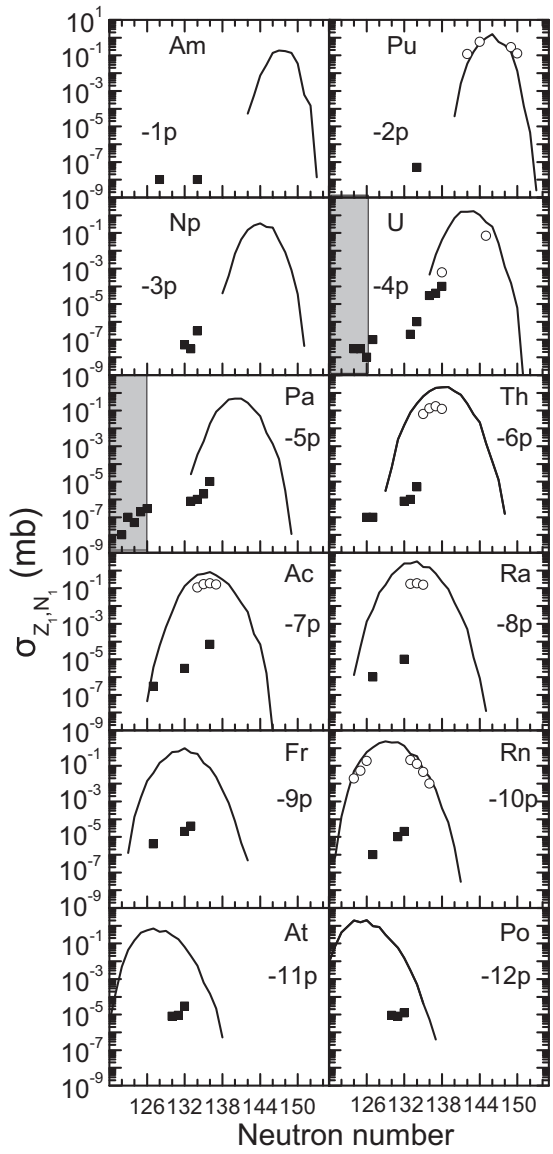

FIG. 2. Transfer cross sections for the ^{48}Ca + ^{248}Cm reaction at $E_{\text{c.m.}} = 226.41$ MeV. The number of transferred protons from ^{48}Ca to ^{248}Cm is indicated. The solid line represents the isotopic distribution cross section of the ultimate product. The solid squares represent experimental data from Refs. [67,68]. The open circle represents experimental data from Ref. [66]. Here, the negative number of transferred nucleons denotes the number of nucleons removed from the projectile.

with high excitation energy are de-excited by evaporating light particles.

In Fig. 2, we also calculated production cross sections of TLF in the reaction ^{48}Ca + ^{248}Cm and compared with the experimental data. The calculated results of the reaction ^{48}Ca + ^{248}Cm at bombarding energy $E_{\text{c.m.}} = 226.41$ MeV are shown by solid lines. It can be seen from Fig. 2 that the calculated transfer cross sections vanish suddenly for the neutron-deficient nuclei in $-1p$ to $-6p$ transfer channels. This is due to the constraints of the present calculation. The calculated potential energy surface by using Eq. (2) is zero when the projectile-like and target-like combinations are located outside the predicted neutron and proton drip lines by macroscopic microscopic model [59].

The experimental transfer cross sections were measured from two different experiments performed at Lawrence Berkeley National Laboratory and GSI (1986 data) [66] for the reaction ^{48}Ca + ^{248}Cm. The experimental data are denoted by open circles in Fig. 2, and they were obtained with radiochemical methods. These methods were limited to identify the fragments of short half-lives and measure the lowest values of transfer cross sections reached to 20 nb. Recently, the experimental data at bombarding energy $E_{\text{c.m.}} = 226.41$ MeV were observed with the velocity filter SHIP at GSI. Some new neutron-deficient nuclei were observed, and the SHIP setup allowed us to search exotic transfer products formed with the cross sections on the 1 nb level. The results are denoted by solid squares (2016 data [67,68]) in Fig. 2. We need to notice that the SHIP can detect the reaction products only in a narrow window of forward angles [67,68]. By comparing the measured experimental data of the same reaction system at similar incident energy involved above, it can be seen that there seems to be a large systematic difference between the sets of experimental data.

Constant distributions for isotopes of Rn through Pu have been measured in the reaction ^{48}Ca + ^{248}Cm in 1986. One can see from Fig. 2 that the 1986 data [66] agree well with predictions made on the basis of improved DNS model+GEMINI++ calculations. Through the 2016 data from $-1p$ to $-6p$ transfer channels, one can see that the model describes the experimental production cross sections of isotopes with $N > 126$ well but deviates from the experimental cross sections for the extremely neutron-deficient Am ($-1p$), U ($-4p$), and Pa ($-5p$) isotopes. In addition, in the data of 2016, the order of magnitude measured by the experimental data [67,68] from $-7p$ to $-9p$ is lower than the calculated results. This discrepancy is obviously large that it cannot be simply explained by uncertainties in the counting efficiencies and statistical error bars. We noticed that the SHIP can detect the reaction products only in a narrow window of forward angles [67,68]. In the present work, however, the total transfer cross section of the ^{48}Ca + ^{248}Cm reaction are predicted with grazing angular momentum for comparison.

The present results of the ^{48}Ca + ^{248}Cm reaction are compared with the predictions of other groups for a wide range of transfers (from $\Delta Z = -1$ to $\Delta Z = -12$). The Dubna model based on the DNS concept combined with a statistical model [68] is adequate for describing the experimental production cross sections of isotopes with $N > 126$ well, but underestimates the cross sections for $N < 126$. We noticed that there are some differences between the present DNS model and the Dubna model to calculate the distribution of primary fragments. The theoretical results of Dubna model were obtained from central collisions with angular momentum $J < 20\hbar$ and a narrow window of forward angles [68]. In the present work, the total transfer cross sections are calculated with grazing angular momentum (see Ref. [69] for more details.). There are also some differences for the description of de-excitation probability. This is because the de-excitation process can be treated within different statistical models. In addition, the

Dubna model normalized the calculated isotopic distributions to the measured isotopic distribution for uranium isotope [68].

There are still some uncertainties to predicted transfer cross sections using the DNS model. The produced neutron-deficient isotopes with the velocity filter SHIP at GSI cannot explain in the above two DNS models combined with the statistical model. On the one hand, the calculated distributions of primary fragments is sensitive to the details of the potential energy surface, it depends on the reliability of the predicted binding energy by the macroscopic-microscopic model and the calculated nucleus-nucleus interaction potential under some assumptions and approximations. In addition, the dynamical potential energy surface has to be further studied by considering the various degrees of freedom. On the other hand, there are some uncertainties for the description of the de-excitation probability, it is related to some nuclear data. For example, for fission barriers of all neutron-deficient nuclides in the region from Bi to U, the analysis of experimental data for the evaporation residue cross sections about 30 projectile-target combinations shows that a decrease in the liquid drop components of the fission barrier by 30–40 % in comparison with the theoretical predictions has a universal character [65].

To compare the production cross sections from the different projectile-target combinations produced the same nuclides through the MNT reaction, we compared the calculated Bi, Po, At, Rn, Fr, Ra, Ac, Th, and Pa isotopes distributions with the experimental data. The results are shown in Fig. 3. These isotopes are produced by transferring several protons and various neutrons from projectile to target for the reaction $^{136}\mathrm{Xe}+{}^{208}\mathrm{Pb}$ at incident energy $E_{\mathrm{c.m.}}=450.00\,\mathrm{MeV}$ [14] and from target to projectile for the reaction $^{48}\mathrm{Ca}+{}^{238}\mathrm{U}$, respectively. It can be seen from Fig. 3 that the isotopic distributions of the $^{48}\mathrm{Ca}+{}^{238}\mathrm{U}$ reaction system above Pb are shifted toward the neutron-rich side as compared to the

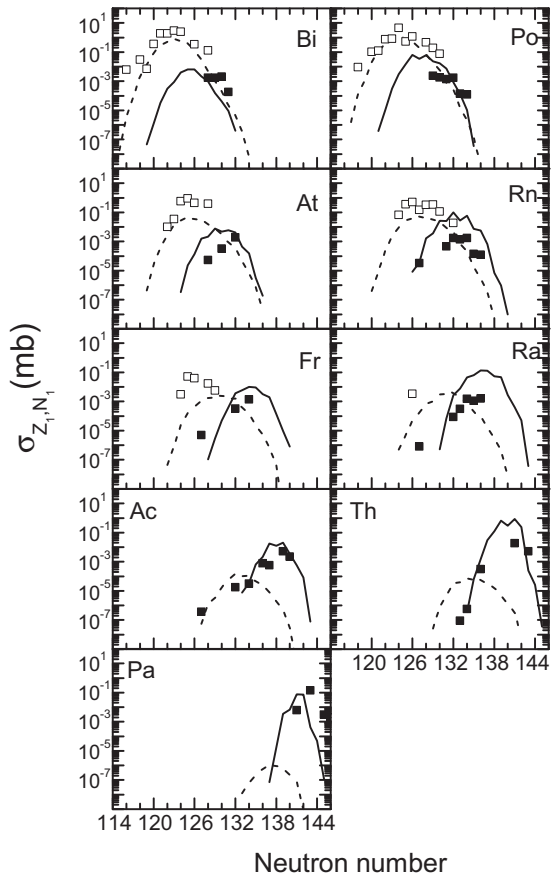

FIG. 3. Comparison of the calculated cross sections between the $^{136}\mathrm{Xe}+{}^{208}\mathrm{Pb}$ reaction and the $^{48}\mathrm{Ca}+{}^{238}\mathrm{U}$ reaction at $Z=83$–91. The calculated cross section of the $^{48}\mathrm{Ca}+{}^{238}\mathrm{U}$ reaction is represented by solid lines, its measured cross section is taken from Ref. [64] and represented by solid square. The calculated cross section of the $^{136}\mathrm{Xe}+{}^{208}\mathrm{Pb}$ reaction is represented by s dashed line, its measured cross section is taken from Ref. [14] and represented by a hollow block.

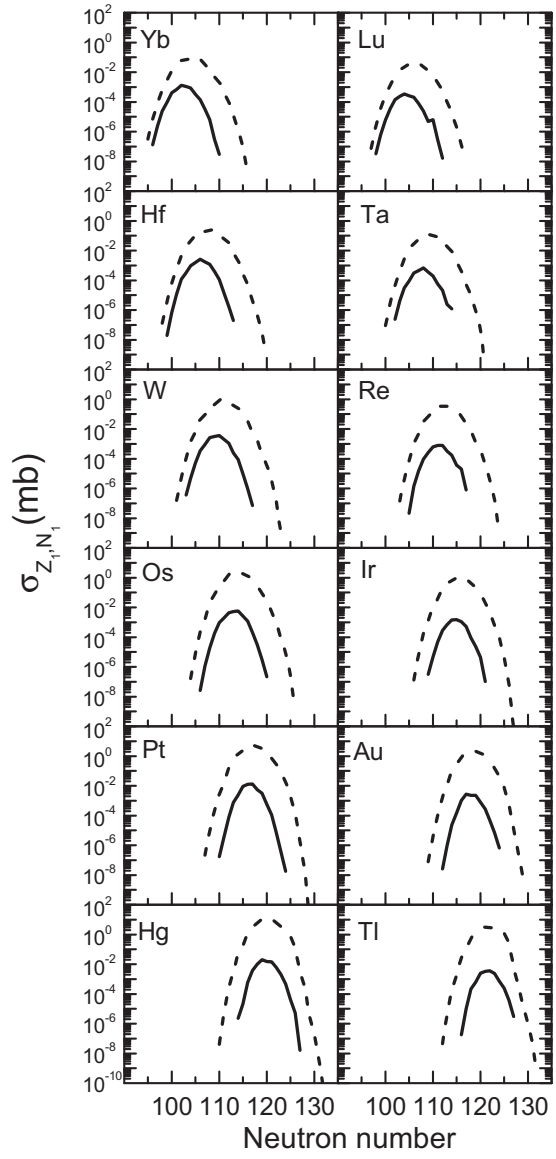

FIG. 4. Comparison of the calculated cross sections between the $^{136}\mathrm{Xe}+{}^{208}\mathrm{Pb}$ reaction and the $^{48}\mathrm{Ca}+{}^{238}\mathrm{U}$ reaction at $Z=70$–81. The solid line represents the calculated cross section for the $^{48}\mathrm{Ca}+{}^{238}\mathrm{U}$ reaction and the dashed line represents the calculated cross section for the $^{136}\mathrm{Xe}+{}^{208}\mathrm{Pb}$ reaction.

^{136}Xe + ^{208}Pb reaction except the isotopic distribution of Bi. From the isotopic distributions above Pb, we find that the reaction ^{48}Ca + ^{238}U tends to favor the production of more neutron-rich nuclei than the reaction ^{136}Xe + ^{208}Pb.

Few experimental data below Pb are available for the ^{48}Ca + ^{238}U reaction, we only compare theoretical values of the isotope distributions for the final fragments for two systems in Fig. 4. One can see from Fig. 4 that the width of the mass distribution of the ^{136}Xe + ^{208}Pb reaction is wider than that of ^{48}Ca + ^{238}U, and the production cross sections for ^{136}Xe + ^{208}Pb overtake the ones of ^{48}Ca + ^{238}U toward the neutron-rich side. The results also showed that the absolute production cross sections of Yb, Lu, Hf, Ta, W, Re, Os, Ir, Pt, Au, Hg, and Tl isotopes, Pb targets lead to about 100–1000 times larger maximum cross sections than U targets for the ^{136}Xe + ^{208}Pb reaction. It is not surprising that about 100–1000 times larger maximum cross sections for MNT products with $Z < 82$ are reached with Pb targets due to Pb is ten protons closer to this region than U.

IV. SUMMARY

The production cross section based on MNT reactions is predicted within an improved DNS model+GEMINI++. The transfer cross sections for the ^{48}Ca + ^{238}U and ^{48}Ca + ^{248}Cm reactions are investigated and compared with the experimental data obtained with the separator for heavy-ion reaction products SHIP at GSI. The theoretical results show that the distributions of isotopes in the ^{48}Ca + ^{238}U reaction are well described within the model. For the ^{48}Ca + ^{248}Cm reaction, there seems to be a large systematic difference between 1986 experimental data and 2016 data. The model partly describes well the experimental production cross sections. Through the 2016 data from $-7p$ to $-12p$ transfer channels, one can see that the experimental cross sections are considerably overestimated with our model. This discrepancy is obviously large that it cannot be simply explained with uncertainties in the counting efficiencies and statistical error bars. The experimental origin of the enhanced cross sections is still an open question.

Experimental and theoretical data from MNT reactions indicate that the reaction ^{48}Ca + ^{238}U tends to favor the production of more neutron-rich nuclei of $Z = 84$–91 than the reaction ^{136}Xe + ^{208}Pb. The calculated results show that the ^{136}Xe + ^{208}Pb reaction leads to the larger cross sections of neutron-rich below Pb isotopes as compared to the reaction ^{48}Ca + ^{238}U.

ACKNOWLEDGMENTS

The work is supported by the National Natural Science Foundation of China (Grants No. 11705055), Hunan Provincial Natural Science Foundation of China (2018JJ3324).

[1] M. Schidel, J. V. Kratz, H. Ahrens, W. Brüchle, G. Franz, H. Gäggeler, I. Warnecke, G. Wirth, G. Herrmann, N. Trautmann, and M. Weis, Phys. Rev. Lett. **41**, 469 (1978).
[2] E. K. Hulet, R. W. Lougheed, J. F. Wild, J. H. Landrum, P. C. Stevenson, A. Ghiorso, J. M. Nitschke, R. J. Otto, D. J. Morrissey, P. A. Baisden, B. F. Gavin, D. Lee, R. J. Silva, M. M. Fowler, and G. T. Seaborg, Phys. Rev. Lett. **39**, 385 (1977).
[3] D. Lee, H. von Gunten, B. Jacak, M. Nurmia, Y.-F. Liu, C. Luo, G. T. Seaborg, and D. C. Hoffmsn, Phys. Rev. C **25**, 286 (1982).
[4] R. Kirchner, O. Klepper, W. Kurcewicz, E. Roeckl, E. Zganjar, E. Runte, W.-D. Schmidt-Ott, P. Tidemand-Petersson, N. Kaffrell, P. Peuser, and K. Rykaczewski, Nucl. Phys. A **378**, 549 (1982).
[5] K. Rykaczewski, R. Kirchner, W. Kurcewicz, D. Schardt, N. Kaffrell, P. Peuser, E. Runte, W.-D. Schmidt-Ott, P. Tidemand-Petersson, and K.-L. Gippert, Z. Phys. A **309**, 273 (1983).
[6] D. C. Hoffman, M. M. Fowler, W. R. Daniels, H. R. von Gunten, D. Lee, K. J. Moody, K. Gregorich, R. Welch, G. T. Sesborg, W. Brüchle, M. Brügger, H. Gaggeler, M. Schadel, K. Sümmerer, G. Wirth, T. Blaich, G. HerImsnn, N. Hildeband, J. V. Kratz, M. Lerch, and N. Trautmann, Phys. Rev. C **31**, 1763 (1985).
[7] M. Schädel, W. Brüchle, H. Gäggeler, J. V. Krstz, K. Sümmerer, G. Wirth, G. Herrmann, R. Stskemann, G. Tittel, N. Trautmann, J. M. Nitschke, E. K. Hulet, R. W. Lougheed, R. L. Hahn, and R. L. Ferguson, Phys. Rev. Lett. **48**, 852 (1982).
[8] W. Królas, R. Broda, B. Fornal, T. Pawłat, H. Grawe, K. H. Maier, M. Schramm, and R. Schubart, Nucl. Phys. A **724**, 289 (2003).
[9] L. Corradi, G. Pollarolo, and S. Szilner, J. Phys. G **36**, 113101 (2009).
[10] W. Loveland, A. M. Vinodkumar, D. Peterson, and J. P. Greene, Phys. Rev. C **83**, 044610 (2011).
[11] J. Kurcewicz, F. Farinon, H. Geissel *et al.*, Phys. Lett. B **717**, 371 (2012).
[12] E. M. Kozulin, E. Vardaci, G. N. Knyazheva *et al.*, Phys. Rev. C **86**, 044611 (2012).
[13] J. V. Kratz, M. Schädel, and H. W. Gäggeler, Phys. Rev. C **88**, 054615 (2013).
[14] J. S. Barrett, W. Loveland, R. Yanez, S. Zhu, A. D. Ayangeakaa, M. P. Carpenter, J. P. Greene, R. V. F. Janssens, T. Lauritsen, E. A. McCutchan, A. A. Sonzogni, C. J. Chiara, J. L. Harker, and W. B. Walters, Phys. Rev. C **91**, 064615 (2015).
[15] Y. X. Watanabe, Y. H. Kim *et al.*, Phys. Rev. Lett. **115**, 172503 (2015).
[16] H. M. Devaraja, S. Heinz, O. Beliuskina *et al.*, Phys. Lett. B **748**, 199 (2015).
[17] D. C. Rafferty, M. Dasgupta *et al.*, Phys. Rev. C **94**, 024607 (2016).
[18] T. Mijatovic, S. Szilner, L. Corradi, D. Montanari, G. Pollarolo, E. Fioretto, A. Gadea, A. Goasduff, D. J. Malenica, N. Marginean, M. Milin, G. Montagnoli, F. Scarlassara, N. Soic, A. M. Stefanini, C. A. Ur, and J. J. Valiente-Dobon, Phys. Rev. C **94**, 064616 (2016).
[19] T. Welsh, W. Loveland, R. Yanez *et al.*, Phys. Lett. B **771**, 119 (2017).
[20] E. M. Kozulin, V. I. Zagrebaev, G. N. Knyazheva *et al.*, Phys. Rev. C **96**, 064621 (2017).
[21] V. V. Desai, W. Loveland, K. McCaleb *et al.*, Phys. Rev. C **99**, 044604 (2019).
[22] A. Winther, Nucl. Phys. A **572**, 191 (1994); **594**, 203 (1995).

[23] V. I. Zagrebaev and Walter Greiner, J. Phys. G: Nucl. Part. Phys **34**, 2265 (2007).
[24] V. I. Zagrebaev and W. Greiner, Phys. Rev. Lett. **101**, 122701 (2008).
[25] V. V. Saiko and A. V. Karpov, Phys. Rev. C **99**, 014613 (2019).
[26] G. G. Adamian, N. V. Antonenko, and A. S. Zubov, Phys. Rev. C **71**, 034603 (2005).
[27] G. G. Adamian, N. V. Antonenko, V. V. Sargsyan, and W. Scheid, Phys. Rev. C **81**, 024604 (2010).
[28] K. Zhao, Z. Li, N. Wang, Y. Zhang, Q. Li, Y. Wang, and X. Wu, Phys. Rev. C **92**, 024613 (2015).
[29] C. Li, F. Zhang, J. Li, L. Zhu, J. Tian, N. Wang, and F. S. Zhang, Phys. Rev. C **93**, 014618 (2016).
[30] N. Wang and Lu Guo, Phys. Lett. B **760**, 236 (2016).
[31] L. Zhu, Z. Q. Feng, and F. S. Zhang, J. Phys. G: Nucl. Part. Phys. **42**, 085102 (2015).
[32] L. Zhu, J. Su, W. J. Xie, and F. S. Zhang, Phys. Rev. C **94**, 054606 (2016).
[33] Z. Q. Feng, Phys. Rev. C **95**, 024615 (2017).
[34] L. Zhu, J. Su, W. J. Xie, and F. S. Zhang, Phys. Lett. B **767**, 437 (2017).
[35] K. Sekizawa and K. Yabana, Phys. Rev. C **88**, 014614 (2013).
[36] K. Sekizawa, Phys. Rev. C **96**, 041601(R) (2017).
[37] K. Godbey, C. Simenel, and A. S. Umar, Phys. Rev. C **101**, 034602 (2020).
[38] X. Jiang and N. Wang, Phys. Rev. C **101**, 014604 (2020).
[39] L. Guo, C. Simenel, L. Shi, and C. Yu, Phys. Lett. B **782**, 401 (2018).
[40] Z. J. Wu and L. Guo, Phys. Rev. C **100**, 014612 (2019).
[41] V. I. Zagrebaev and W. Greiner, Nucl. Phys. A **944**, 257 (2015).
[42] Z. Q. Feng, G. M. Jin, and J. Q. Li, Phys. Rev. C **80**, 067601 (2009).
[43] A. V. Karpov and V. V. Saiko, Phys. Rev. C **96**, 024618 (2017).
[44] Y. E. Penionzhkevich, G. G. Adamian, and N. V. Antonenko, Phys. Lett. B **621**, 119 (2005).
[45] Y. E. Penionzhkevich, G. G. Adamian, and N. V. Antonenko, Eur. Phys. J. A **27**, 187 (2006).
[46] S. Ayik, B. Yilmaz, O. Yilmaz, and A. S. Umar, Phys. Rev. C **100**, 014609 (2019).
[47] S. Ayik, B. Yilmaz, O. Yilmaz, A. S. Umar, and G. Turan, Phys. Rev. C **96**, 024611 (2017).
[48] S. Ayik, B. Yilmaz, O. Yilmaz, and A. S. Umar, Phys. Rev. C **97**, 054618 (2018).
[49] X. Jiang and N. Wang, Chin. Phys. C **42**, 104105 (2018).
[50] F. S. Zhang, C. Li, L. Zhu, and P. W. Wen, Front. Phys. **13**, 132113 (2018).
[51] C. Li, C. A. T. Sokhna, X. Xu, J. Li, G. Zhang, B. Li, Z. Ge, and F.-S. Zhang, Phys. Rev. C **99**, 034619 (2019).
[52] R. Yanez and W. Loveland, Phys. Rev. C **91**, 044608 (2015).
[53] P. W. Wen, A. K. Nasirov, C. J. Lin, and H. M. Jia, J. Phys. G: Nucl. Part. Phys. **47**, 075106 (2020).
[54] X. J. Bao, S. Q. Guo, H. F. Zhang, and J. Q. Li, Phys. Rev. C **97**, 024617 (2018).
[55] X. J. Bao, Phys. Rev. C **102**, 054613 (2020).
[56] S. Q. Guo, X. J. Bao, H. F. Zhang, J. Q. Li, and N. Wang, Phys. Rev. C **100**, 054616 (2019).
[57] S. Ayik, B. Schürmann, and W. Nörenberg, Z. Phys. A **277**, 299 (1976).
[58] S. Ayik, G. Wolschin, and W. Nörenberg, Z. Phys. A **286**, 271 (1978).
[59] N. Wang, M. Liu, and X. Wu, Phys. Rev. C **81**, 044322 (2010).
[60] S. Q. Guo, Y. Gao, J. Q. Li, and H. F. Zhang, Phys. Rev. C **96**, 044622 (2017).
[61] http://bitbucket.org/arekfu/gemini/src/master/.
[62] R. J. Charity, Phys. Rev. C **82**, 014610 (2010).
[63] D. Mancusi, R. J. Charity, and J. Cugnon, Phys. Rev. C **82**, 044610 (2010).
[64] H. M. Devaraja, S. Heinz, D. Ackermann, T. Göbel, F. P. Hebberger, S. Hofmann, J. Maurer, G. Münzenberg, A. G. Popeko, A. V. Yeremin, Eur. Phys. J. A **56**, 224 (2020).
[65] A. V. Yeremin, Phys. Part. Nucl. **38**, 492 (2007).
[66] H. Gäggeler, W. Brüchle, M. Brügger, M. Schädel, K. Sümmerer, G. Wirth, J. V. Kratz, M. Lerch, T. Blaich, G. Herrmann, N. Hildebrand, N. Trautmann, D. Lee, K. J. Moody, K. E. Gregorich, R. B. Welch, G. T. Seaborg, D. C. Hoffman, W. R. Daniels, M. M. Fowler, and H. R. von Gunten, Phys. Rev. C **33**, 1983 (1986).
[67] S. Heinz *et al.*, Eur. Phys. J. A **52**, 278 (2016).
[68] Sh. A. Kalandarov, G. G. Adamian, N. V. Antonenko, H. M. Devaraja, and S. Heinz, Phys. Rev. C **102**, 024612 (2020).
[69] X. J. Bao, Nucl. Phys. A **986**, 60 (2019).